2021

Antioxidant activity of thunbergia laurifolia lindl. Ethanolic extract in keratinocytes

Buakotchaphan Jirabanjerdsiri
Faculty of Pharmaceutical Sciences

ANTIOXIDANT ACTIVITY OF *THUNBERGIA LAURIFOLIA* LINDL. ETHANOLIC EXTRACT IN KERATINOCYTES

Miss Buakotchaphan Jirabanjerdsiri

A Thesis Submitted in Partial Fulfillment of the Requirements
for the Degree of Master of Science in Pharmaceutical Sciences and Technology
FACULTY OF PHARMACEUTICAL SCIENCES
Chulalongkorn University
Academic Year 2021

ฤทธิ์ต้านออกซิเดชันของสารสกัดเอทานอลจากรางจืดในเซลล์เคอราติโนไซต์

น.ส.บัวกชพรรณ จิรบรรเจิดสิรี

วิทยานิพนธ์นี้เป็นส่วนหนึ่งของการศึกษาตามหลักสูตรปริญญาวิทยาศาสตรมหาบัณฑิต
สาขาวิชาเภสัชศาสตร์และเทคโนโลยี ไม่สังกัดภาควิชา/เทียบเท่า
คณะเภสัชศาสตร์ จุฬาลงกรณ์มหาวิทยาลัย
ปีการศึกษา 2564

Thesis Title	ANTIOXIDANT ACTIVITY OF *THUNBERGIA LAURIFOLIA* LINDL. ETHANOLIC EXTRACT IN KERATINOCYTES
By	Miss Buakotchaphan Jirabanjerdsiri
Field of Study	Pharmaceutical Sciences and Technology
Thesis Advisor	Professor SUCHADA SUKRONG, Ph.D.
Thesis Co Advisor	Professor PITHI CHANVORACHOTE, Ph.D.

Accepted by the FACULTY OF PHARMACEUTICAL SCIENCES, Chulalongkorn University in Partial Fulfillment of the Requirement for the Master of Science

..... Dean of the FACULTY OF PHARMACEUTICAL SCIENCES

(Professor PORNANONG ARAMWIT, Ph.D.)

THESIS COMMITTEE

..... Chairman

(Associate Professor SORNKANOK VIMOLMANGKANG, Ph.D.)

..... Thesis Advisor

(Professor SUCHADA SUKRONG, Ph.D.)

..... Thesis Co-Advisor

(Professor PITHI CHANVORACHOTE, Ph.D.)

..... Examiner

(Assistant Professor PREEDAKORN CHUNHACHA, Ph.D.)

..... External Examiner

(Associate Professor Potchanapond Graidist, Ph.D.)

บัวกชพรรณ จิรบรรเจิดสิรี : ฤทธิ์ต้านออกซิเดชันของสารสกัดเอทานอลจากรางจืดในเซลล์เคอราติโนไซต์. (ANTIOXIDANT ACTIVITY OF *THUNBERGIA LAURIFOLIA* LINDL. ETHANOLIC EXTRACT IN KERATINOCYTES) อ.ที่ปรึกษาหลัก : ศ. ภญ. ร.ต.อ.หญิง ดร. สุชาดา สุขหร่อง, อ.ที่ปรึกษาร่วม : ศ. ภก. ดร.ปิติ จันทร์วรโชติ

ฝุ่นละอองขนาดเล็กกว่า 2.5 ไมครอน (พีเอ็ม 2.5) สามารถทำให้ผิวหนังเสียหายผ่านการเหนี่ยวนำภาวะเครียดออกซิเดชันในผิวหนังชั้นนอก สารต้านอนุมูลอิสระช่วยต้านอนุมูลอิสระและรักษาสภาวะสมดุลของเซลล์ การศึกษานี้มีวัตถุประสงค์ในการศึกษาประสิทธิภาพการป้องกันของสารสกัดเอทานอลจากรางจืดต่อภาวะเครียดออกซิเดชันเหนี่ยวนำโดยพีเอ็ม 2.5 ในเซลล์เคอราติโนไซต์ของผิวหนัง ตรวจวัดปริมาณกรดโรสมารินิกในสารสกัดด้วยโครมาโทกราฟีเหลวสมรรถนะสูงพร้อมการตรวจจับอาร์เรย์ไดโอด ตรวจความอยู่รอดของเซลล์ด้วยสาร 3-(4,5-ไดเมทิลไทอะซอล-2-อิล)-2,5-ไดฟีนิลเตตราโซเลียม โบรไมด์ ติดตามอนุมูลอิสระภายในเซลล์โดยสาร 2',7'-ไดคลอโรไดไฮโดรฟลูออเรสซีน ไดอะซีเตต วิเคราะห์โปรตีนที่เกี่ยวข้องกับกระบวนการส่งทอดสัญญาณพี62-คีพ1-เอ็นอาร์เอฟ2 โดยเวสเทอร์นบล็อท ตรวจสอบการแสดงออกของเอ็นอาร์เอฟ 2 และพี 62 เพิ่มเติมด้วยปฏิกิริยาอิมมูนเรืองแสง การเลี้ยงเซลล์ด้วยพีเอ็ม 2.5 ที่ความเข้มข้นซึ่งไม่เป็นพิษต่อเซลล์สามารถกระตุ้นการสร้างอนุมูลอิสระได้ภายใน 6 ชั่วโมง การเลี้ยงเซลล์ด้วยสารสกัดรางจืดและพีเอ็ม 2.5 เป็นเวลา 6 ชั่วโมง สามารถยับยั้งการสร้างอนุมูลอิสระส่วนเกินที่กระตุ้นโดยพีเอ็ม 2.5 ได้อย่างมาก นอกจากนี้สารสกัดรางจืดช่วยเสริมการป้องกันของเซลล์เคอราติโนไซต์ผ่านการเพิ่มระดับของโปรตีนพี 62, เอ็นอาร์เอฟ 2, และเอสโอดี 1 สารสกัดรางจืดเพิ่มความเสถียรของโปรตีนเอ็นอาร์เอฟ 2 และพี 62 ในขณะที่ยับยั้งการแสดงออกของคีพ 1 โดยสรุปแล้วสารสกัดรางจืดเป็นสารต้านอนุมูลอิสระจากธรรมชาติที่มีประสิทธิภาพในการต้านภาวะเครียดออกซิเดชันที่เกิดจากพีเอ็ม 2.5 ในเซลล์เคอราติโนไซต์

สาขาวิชา	เภสัชศาสตร์และเทคโนโลยี	ลายมือชื่อนิสิต .....
ปีการศึกษา	2564	ลายมือชื่อ อ.ที่ปรึกษาหลัก .....
		ลายมือชื่อ อ.ที่ปรึกษาร่วม .....

6272006233 : MAJOR PHARMACEUTICAL SCIENCES AND TECHNOLOGY
KEYWORD: keratinocytes, PM2.5, Thunbergia laurifolia, antioxidants, Nrf2, p62, air pollution, particulate matter

Buakotchaphan Jirabanjerdsiri : ANTIOXIDANT ACTIVITY OF *THUNBERGIA LAURIFOLIA* LINDL. ETHANOLIC EXTRACT IN KERATINOCYTES. Advisor: Prof. SUCHADA SUKRONG, Ph.D. Co-advisor: Prof. PITHI CHANVORACHOTE, Ph.D.

Fine particulate matter ($PM_{2.5}$) can cause skin damage through the induction of oxidative stress in epidermis. Antioxidants help counteract with cellular oxidant species and maintain cell homeostasis. This study aims to examine the protective effect of *Thunbergia laurifolia* lindl. ethanolic extract on $PM_{2.5}$-mediated oxidative stress in epidermal keratinocytes. High-performance liquid chromatography with diode array detection was conducted for quantitative analysis of rosmarinic acid content in the extract. Cell viability was detected by the 3-(4,5-Dimethylthiazol-2-yl)-2,5-Diphenyltetrazolium Bromide assay. Intracellular ROS was monitored using 2',7'-Dichlorodihydrofluorescein diacetate. Proteins related to p62-Keap1-Nrf2 signaling pathway were examined by western blot analysis. Expressions of Nrf2 and p62 were further determined by immunofluorescence. $PM_{2.5}$ treatment at non-cytotoxic concentration could remarkably induce reactive oxygen species (ROS) production within 6 h. The co-treatment of the extract and $PM_{2.5}$ for 6 h dramatically inhibited excess ROS production induced by $PM_{2.5}$. In addition, the extract enhanced cellular defense of keratinocytes, by increasing the levels of p62, Nrf2 and SOD1 proteins. The extract stabilizes Nrf2 and p62 expressions, while suppresses Keap1 expression. The *T. laurifolia* extract is promising natural antioxidants against oxidative stress induced by $PM_{2.5}$ in keratinocytes.

Field of Study:	Pharmaceutical Sciences and Technology	Student's Signature .....
Academic Year:	2021	Advisor's Signature .....
		Co-advisor's Signature .....

ACKNOWLEDGEMENTS

Firstly, I am so grateful to my advisor and co-advisor, Professor Suchada Sukrong (Ph.D.) and Professor Pithi Chanvorachote (Ph.D.), respectively, for always providing great opportunity and support, professional advices and supervision during my study in Chulalongkorn University.

Furthermore, I am sincerely appreciate the tuition fee scholarship from the graduate school, Chulalongkorn University to commemorate the 72nd anniversary of his Majesty King Bhumibol Aduladej. My special thanks are extended to all co-authors in my publication, for there contribution, helpful guidance, valuable discussion and criticism. Especially, Associate Professor Dr. Tassanee Prueksasit of Department of Environmental Science, Faculty of Science, Chulalongkorn University for special advices and support in air pollution and PM2.5 sampler collection.

I am also thankful to all of my laboratory partners at Center of Excellence in DNA Barcoding of Thai Medicinal Plants and Center of Excellence in Cancer Cell and Molecular Biology for their supportive advices and training.

Buakotchaphan Jirabanjerdsiri

TABLE OF CONTENTS

List of figures

Page

CHAPTER I

INTRODUCTION

1.1 Background and rational

Skin is responsible for innate immunity providing first line defense against external hazards such as microbes, physical and chemical stimuli, and ultraviolet (UV) radiation. Skin protection relies on skin barrier regulated by keratinocytes in the outermost layer. Skin barrier prevents physical harmful invasion and penetration of foreign substances[1]. Prolonged oxidative stress will eventually initiate apoptotic and necrotic of keratinocytes and depletion of antioxidants. The destruction and impairment of keratinocytes will increase skin susceptibility to infection, aggravate many skin diseases, and lead to undesirable skin aging and skin cancer[2].

Air pollution has been increased in recent years because of industrialization[3]. Particulate matter (PM) affects human health and contributes to several pathological conditions. Among several size of PM, $PM_{2.5}$, fine particle with diameter smaller than 2.5 μm, can penetrate the lung tissue and skin barrier aggravating the respiratory, cardiovascular, and skin diseases[4]. Traffic $PM_{2.5}$, obtained from gasoline and diesel vehicles emission, contains the most toxic substances towards skin. It consists of inorganic compounds (heavy metals especially Zn, Cu, and Fe) and organic

compounds especially polycyclic aromatic hydrocarbons (PAHs)[5]. It is vital to maintain healthy skin barrier as skin provides first line defense against external hazards. The exposure of keratinocytes to $PM_{2.5}$ induces oxidative stress[6]. Oxidative stress occurs when antioxidants reservoir in keratinocytes unable to maintain redox homeostasis resulting from excess reactive oxygen species (ROS) production which can lead to apoptosis, early skin aging, and keratinocyte carcinoma[7]. In general, keratinocytes counteract stimulated oxidants by Kelch-like ECH-associated protein 1 (Keap1)-Nuclear factor erythroid 2-related factor (Nrf2) pathway[8]. In normal condition, Nrf2 forms dimerization with Keap1 and constantly induce Nrf2 degradation[9]. The p62 protein can sequester Keap1 from Nrf2-Keap1 dimer and consequently induces p62-Keap1 degradation. The released Nrf2 then translocate into nucleus to activate antioxidant responsive elements (ARE) and transactivates antioxidant and detoxifying enzymes such as SOD1 and CAT[10]. Interestingly, an overexpression of p62 prolongs Nrf2 activity as cells take time to degrade p62-Keap1 accumulation and transactivate antioxidant and detoxifying genes to restore homeostasis[11].

The leaves of *Thunbergia laurifolia* Lindl., a woody climbing plant belongs to the Acanthaceae family typically grows in Southeast Asia, has been used as an alternative medicine for detoxifying[12] and antioxidant properties[13]. According to previous high-performance liquid chromatography (HPLC) analysis, rosmarinic acid is the major phenolic compound in *T. laurifolia* extract[14]. Recent study indicated that

T. laurifolia ethanolic extract could inhibit lipid peroxidation and scavenge DPPH$^{\bullet}$ radical in chemical reaction experiments[15]. In biological study, the extract could also scavenge nitric oxide and inducible nitric oxide synthase (iNOS) production in RAW264.7 mouse macrophage cells[16]. Furthermore, the extract could inhibit ROS production induces by H_2O_2 in normal human dermal fibroblast cells[16]. Since an underlying cellular antioxidant defense system of *T. laurifolia* extract (TLE) against $PM_{2.5}$ in keratinocytes has not been investigated, this study aims to evaluate cellular antioxidant defense system of TLE against $PM_{2.5}$-oxidative stress induction in keratinocytes. The effects of the extract and $PM_{2.5}$ on cell viability, ROS production, and p62-Keap1-Nrf2 signaling pathway were examined.

1.2 Objectives

1) To evaluate the protective effect of *T. laurifolia* ethanolic extract against $PM_{2.5}$-induced oxidative stress in keratinocytes.

2) To examine effect of *T. laurifolia* ethanolic extract on cellular antioxidant defense system in keratinocytes.

1.3 Hypothesis

An *in vitro* study of *T. laurifolia* ethanolic extract in keratinocytes might reveal potent antioxidant activity through upregulating Nrf2 signaling pathway against $PM_{2.5}$-induced oxidative stress.

1.4 Expected benefit of the study

To obtain *T. laurifolia* ethanolic extract with antioxidant activity which could inhibit oxidative stress induced by $PM_{2.5}$ in keratinocytes. The extract might provide cytoprotective effect and help to strengthen skin barrier. This potent natural antioxidants might be able to apply in cosmetic and pharmaceutical industry.

1.5 Conceptual framework

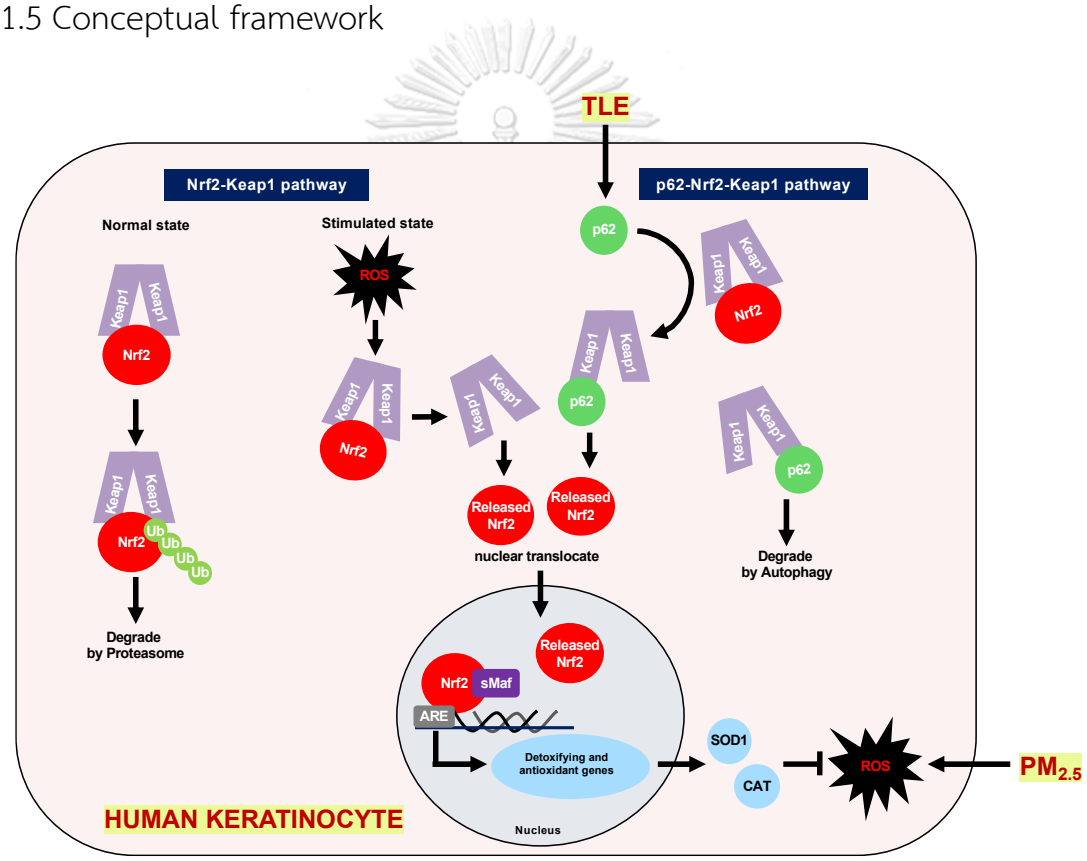

Figure 1 Conceptual framework

1.6 Experimental design

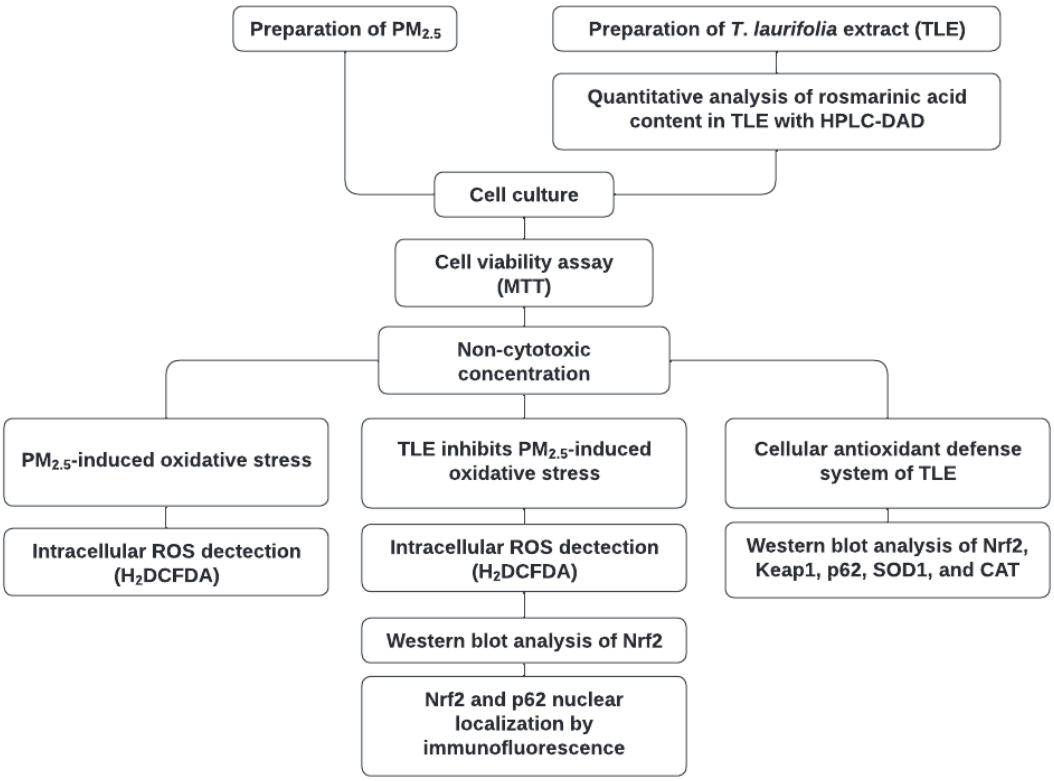

CHAPTER II

LITERATURE REVIEW

2.1 Skin

Skin is the largest organ covering external surface of human body. One of the vital roles of skin is providing first line defense against foreign substances and environmental hazards: chemical and physical stimuli, microorganisms, and ultraviolet (UV) radiation. Skin composes of three main layers; epidermis, dermis, and hypodermis[1].

Epidermis

Epidermis is the outermost layer of skin. Epidermis is associated with innate immunity as it provides a protective barrier from external stimuli. This skin layer composed of keratinocytes, melanocytes, Merkel's cell and Langerhans cells[2].

Keratinocytes dominate epidermis as it constantly proliferated, differentiated, and migrated from basal cells located in stratum germinativum, the basal layer. Keratinocytes undergo cornification and desquamation throughout basal layer to the upper layer creating three more layers above: stratum spinosum (SP), stratum granulosum (SG), and stratum corneum (SC), respectively. Keratinocytes took approximately 14 days to transit from basal layer to SC and another 14 days to turnover within SC. To conclude, it took 14 days to replace SC and 28 days to

replace the entire epidermis in normal condition. In certain state like inflammation or hyperproliferative diseases might affects the turnover times[17]. Normally, SC, the uppermost layer of epidermis, support skin barrier with extracellular lipids (hydrolipid film) overlay SC. This hydrolipidic layer prevent skin invasion and penetration. In SC, the rigid nonviable keratinocytes is known as corneocytes. The settlement of corneocytes amongst intercellular lipids can theoretically portrays 'brick and mortar' model as shown in figure 2. The degradation of corneodesmosomes (protein linkages between corneocytes) create lacunar spaces consequently construct aqueous pore pathway in SC[18].

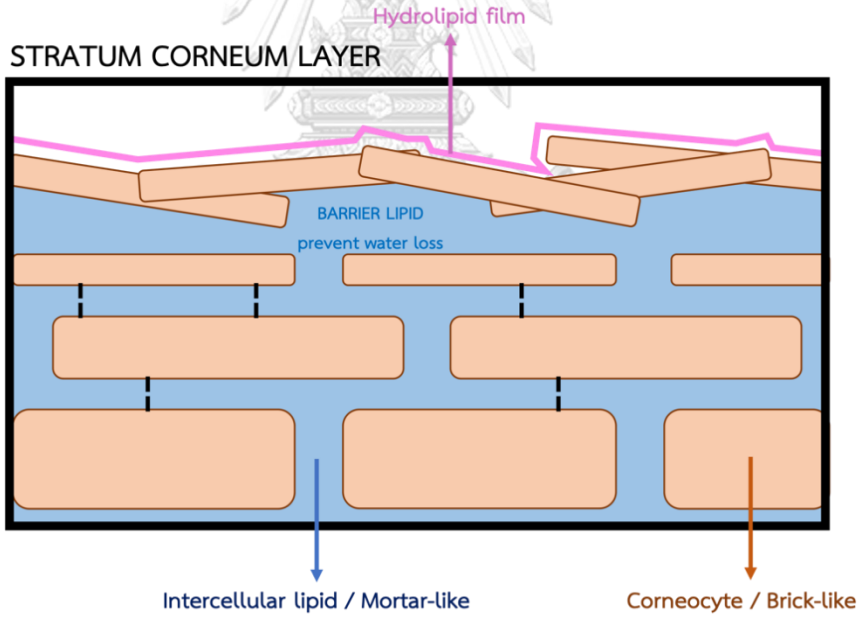

Figure 2 Brick-and-mortar-like model

This model composed of rigid nonviable corneocytes (brick-like) orderly align amongst intercellular lipids (mortar-like). Corneodesmosomes (black dashed line) provide intercellular adhesion in stratum corneum layer. The intercellular

membranes maintain skin moisture. In normal condition, hydrolipid film that overlay the stratum corneum provides skin protection against invasion and penetration.

Melanocytes are dendritic cells that synthesize skin pigments. They mainly settle in the basal layer. Furthermore, Merkel cells functioning as mechanoreceptors also located in the basal layer. Langerhans cells (LCs), another dendritic cells or macrophages, composed 2-8% of epidermis found mostly in SP. LCs form network across the epidermis guarding immune system. Enabling connection between innate and adaptive immunity. They regulate appropriate adaptive immune response when encounter foreign bodies; switching between immune activation and immune tolerance. For instance, during infection or wound LCs can stimulate T lymphocytes for protective immunity[19].

Dermis

Dermis is the middle layer of skin. Dermis engage in skin elasticity and tension strength providing skin support and protection against mechanical injury, thermoregulation, and sensation. Dermis can be divided into two layers: the papilla dermis (PD) and the reticular dermis (RD). PD is the superficial layer composed of loose connective tissue like collagen and elastic fibers with blood vessels and nerves supplied. This vascular network is responsible for inflammatory response by recruit neutrophils, lymphocytes, and other inflammatory cells. The deeper layer RD formed thick layer of dense connective tissue like thick elastic fibers.

Certain types of cell can be found within the connective tissue of dermis including adipocytes, fibroblasts, macrophages, mast cells, Schwann cells, and stem cells[20]. Fibroblasts are the main cell type that synthesis collagen, elastic fibers and extracellular matrix material. Adipocytes aid superficial arteriovenous plexus in body temperature regulation. They form insulating barrier to prevent heat loss. Also enhance wound healing process. Dermis also houses skin appendages include arrector pili muscles, blood and lymphatic vessels, hair, hair follicles, sensory neurons and sweat glands. Several nerve endings around hair follicles and mechanoreceptors allow skin sensation like hair movement, pressure and vibration.

Hypodermis

Hypodermis is the innermost and thickest layer of skin. It also known as subcutaneous tissue. It composed of adipose tissue that serves insulation and energy reservoir. Hypodermis houses skin appendages like hair follicles, sensory neurons, and blood vessels[2].

2.2 Nrf2 modulate skin protection

Skin protection mainly depend on the skin barrier of stratum corneum. Keratinocytes plays a vital role in the innate immunity. The disruption or dysfunction of keratinocytes increases skin susceptibility to infection that can aggravate skin

diseases such as atopic dermatitis[21]. Impaired skin barrier could not fully protect skin against harmful foreign substances.

In general, skin is damaged from intracellular reactive oxygen species (ROS) generating during cellular metabolism especially melanosynthesis and immunometabolism. The external factors including ultraviolet (UV) radiation, air pollutants, physical and chemical hazards, and microorganisms. All of these factors deplete skin antioxidants and produce excess ROS. Eventually cause undemanding oxidative stress. The prolonged oxidative stress constantly damaged cellular compartments include carbohydrates, lipids, nucleic acids, and proteins. Adverse effects resulting from oxidative stress include apoptotic and necrotic cells, early skin aging, and skin cancer[22]. However, skin cells have sophisticated self-defense mechanism against oxidative stress: nuclear factor erythroid 2-related factor 2 (Nrf2)-mediated pathway[23]. As Nrf2 binds to antioxidant responsive elements (ARE), it enhances genes expression of Phase II detoxifying/antioxidant enzymes in response to oxidative stress.

The activation pathway of Nrf2 can be divided into two ways including Nrf2-Keap1 pathway and p62-Keap1-Nrf2 pathway. For Nrf2-Keap1 pathway, the quantity of Nrf2 in cytoplasm is regulated by cytoplasmic protein named Kelch-like ECH-associated protein 1 (Keap1) in normal condition. Keap1 is an adaptor protein for cullin 3 (Cul3) dependent E3 ubiquitin ligase complex that electrophiles targeted for inhibition. The binding of Nrf2-Keap1-Cul3 complex rapidly degrade Nrf2 through

proteasome pathway. The complex binding eventually ubiquitylates Nrf2 at lysine residue. An ubiquitylated Nrf2 is then transformed to 26S proteasomes to proceed degradation as shown in figure 3.

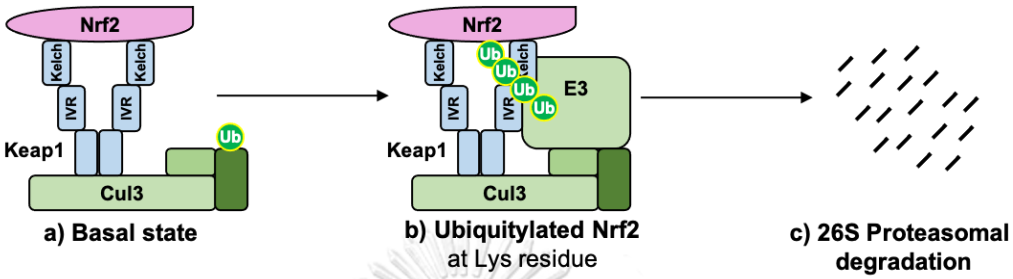

Figure 3 A model displays Nrf2 and Keap1 interaction in basal state

a) At basal state, two Keap1 molecules form homodimer and bind to Cullin3. Dimeric Keap1 molecules seize Nrf2 molecule through Kelch domains forming Nrf2-Keap1-Cul3 complex. **b)** Under non-stress conditions, the Cul3 complex ubiquitylates Nrf2 at lysine residue. **c)** Ubiquitylated Nrf2 is then transformed to 26S proteasomes to proceed degradation.

Meanwhile under oxidative stress, oxidants can modify Keap1 conformation by oxidation of the cysteine residues in Keap1. The modification of Keap1 dissociated the Nrf2-Keap1-Cul3 complex[24]. The released Nrf2 can translocate into the nucleus. Nrf2 must be formerly bound to small musculoaponeurotic fibrosarcoma (sMaf) proteins then enable to bind to ARE in DNA promoter region, and consequently initiate antioxidant genes transcription as seen in figure 4[25]. Phase II detoxifying/antioxidant enzymes such as catalase (CAT), glutathione S-transferase

(GST), heme oxygenase-1 (HO-1), superoxide dismutase (SOD), and etc.[26]. Therefore, the activation of Nrf2 dissociated from Nrf2-Keap1-Cul3 complex dramatically protect keratinocytes throughout differentiation, and even prevent carcinogenesis[27].

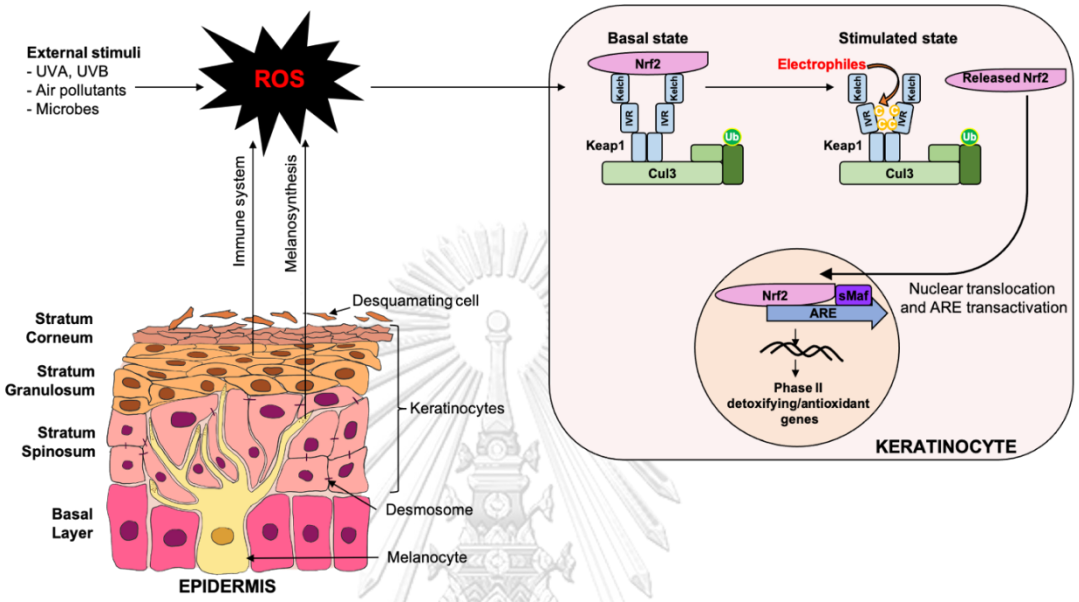

Figure 4 Nrf2-mediated pathway in human epidermal keratinocyte

In general, ROS is generated from cellular metabolism such as immunometabolism and melanosynthesis. Further skin explosion to external stimuli includes UV radiation, air pollutants, and microbes also stimulate ROS production led to stimulation of Nrf2 in keratinocyte[28]. Nrf2-mediated pathway is sophisticated cell defense against oxidative stress. Electrophiles like oxidants oxidize cysteine residues in Keap1 that result in conformation of Keap1, and dissociation of Nrf2. Released Nrf2 then translocate into nucleus and bind to sMaf prior to ARE transactivation. Then initiate Phase II detoxifying/antioxidant genes expression[9].

In general, superoxide anion within cells is rapidly converted into H_2O_2 by superoxide dismutases 1 and 2 (SOD1 and 2). In this study model, will focus on SOD1 that is mainly located in the cytosol and mitochondrial matrix which associated to external oxidative stress stimuli[29]. Furthermore, H_2O_2 can be converted to H_2O by cellular antioxidant protein such as catalase (CAT) in order to prevent hydroxyl radicals generated from excess H_2O_2 in the presence of ferrous ions by the Fenton reaction [30].

In p62-Keap1-Nrf2 pathway, the p62 protein with higher binding affinity sequesters Keap1 from Nrf2-Keap1 dimer. The p62-Keap1 complex consequently undergoes autophagic degradation in the cytosol with p62 mediation. The released Nrf2 then translocate into nucleus to activate antioxidant responsive elements (ARE) and transactivates antioxidant and detoxifying enzymes such as SOD1 and CAT[10]. Interestingly, an accumulation of p62-Keap1 complex prolongs Nrf2 activity as cells take time to degrade p62-Keap1 accumulation and generate antioxidant and detoxifying genes to rebalance homeostasis[11].

2.3 $PM_{2.5}$

There are about 99% of global population facing poor air quality with extreme air pollution according to World Health Organization (WHO)'s recent database in 2019[31]. The most recent data in 2016 states that poor ambient air

quality in the cities and rural areas caused premature deaths in 4.2 million people. The premature deaths majorly occurred in low- and middle-income countries especially in South-East Asia and Western Pacific regions.

Air pollution plays a vital role in induction and aggravation of cardiovascular and respiratory diseases, and cancers. Amongst the 4.2 million premature deaths approximately 58% were due to ischemic heart disease and stroke. The others 18% and 6% of premature deaths were resulting from respiratory diseases and lung cancer, respectively. Interestingly, household air pollution, cooking and heat generated from biomass fuels and coal, is the major source of ambient air pollution[31]. WHO has indicated global air quality guideline level for $PM_{2.5}$ concentration in the air should be less than 5 $\mu g/m^3$ for long-term exposure and 15 $\mu g/m^3$ for 3-4 exceedance days per year. However, WHO has also set four interim targets as steps to reduce air pollutant levels.

Air pollutants can be classified into 4 groups.

1) **Gaseous pollutants** such as ozone, carbon monoxide, and volatile organic compounds.
2) **Persistent organic pollutants** like dioxins.
3) **Heavy metals** including cadmium, lead and mercury.
4) **Particulate matter** (PM)
    a. $PM_{0.1}$ (ultrafine particles) sizing smaller than 0.1 μm.
    b. $PM_{2.5}$ (fine particles) sizing smaller than 2.5 μm.

c. PM_{10} (coarse particles) sizing smaller than 10 μm.

The major source of PM is combustion of fossil fuels using for human transportation and energy generation[4]. Traffic emissions contribute most of the PM. Traffic PM consists of primary particles emitted from an incomplete combustion resulting from abrasion of tires and brakes on road surfaces. Furthermore, it also contains secondary aerosol particles that chemically and physically interact with the primary gaseous pollutants in the atmosphere[32]. The secondary aerosol particles can be grouped into two groups which are secondary organic and inorganic aerosols.

The component of $PM_{2.5}$ can be classified into three groups.

1) **Minerals** generated from chemical and physical reactions such as quartz.
2) **Inorganic compounds** including heavy metals like cadmium, manganese, cobalt and copper.
3) **Organic compounds** produced from primary and secondary sources includes toxic substances like polycyclic aromatic hydrocarbons (PAHs), oxygenated or nitrated PAHs, radicals, and phenols.

Skin permeable $PM_{2.5}$ targets mitochondria. $PM_{2.5}$-damaged mitochondria evokes excess ROS generation leading to oxidative stress and inflammatory cascade[33]. Excess ROS production depletes skin antioxidants disturbing cellular redox homeostasis. ROS damage lipids, proteins, DNA and several cellular compartments[34].

The exposure of $PM_{2.5}$ in keratinocytes stimulates Nrf2 which regulates phase II antioxidant and detoxifying enzymes counteracts the oxidative stress[35]. $PM_{2.5}$ constituents especially organic and inorganic compounds (PAHs and heavy metals, respectively), can induce Nrf2 and AhR signaling pathways (figure 5). Inorganic compounds transport through cell membrane by facilitated diffusion transport proteins. Inorganic compounds target mitochondria resulting in $PM_{2.5}$ accumulation within mitochondria inducing ROS generation. Organic compounds can cross the cell membrane due to their lipophilic characteristic. The organic compounds act as a AhR ligands. The activation of AhR upregulates cytochrome P450 (CYP) and induces proinflammatory responses[28]. ROS generation provokes cellular defense system, Nrf2 signaling pathway. However, the prolonged and constantly exposure of $PM_{2.5}$ can cause mitochondria dysfunction and impaired cellular defense system. The oxidative stress can activate apoptosis, the programmed cell death[7].

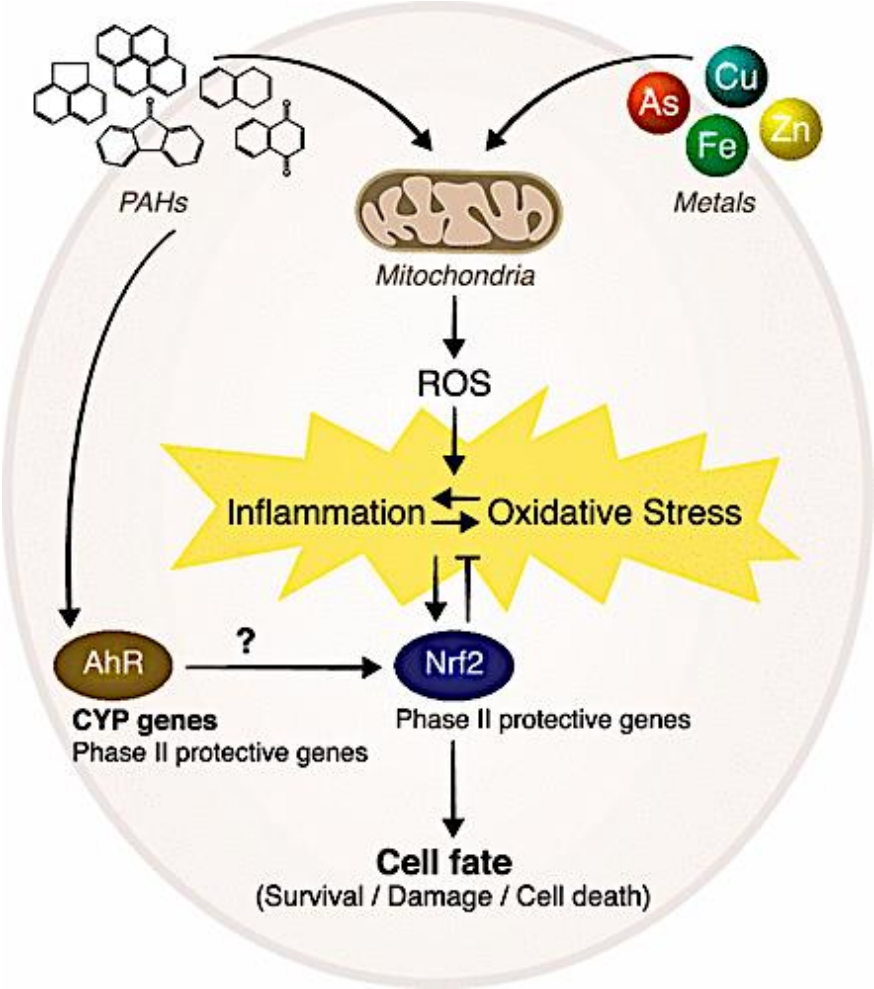

Figure 5 $PM_{2.5}$ induces oxidative stress and inflammation [35]

$PM_{2.5}$ composes of organic and inorganic compounds, (mainly metals and PAHs, respectively), can penetrate cell membrane and target mitochondria. $PM_{2.5}$ induces ROS production and consequently cause oxidative stress and inflammation. The excess ROS production activates Nrf2 signaling pathway in response. In addition, the PAHs component also activates AhR which consequently induces CYP enzymes initiating inflammatory cascade[35].

2.4 *Thunbergia laurifolia* Lindl.

Thunbergia laurifolia Lindl. is a woody climbing plant belongs to the Acanthaceae family. In Thailand, *T. laurifolia* is commonly known as Rang Chuet. This woody climber (figure 6) has simple leaves grow in opposite pairs along the stalk; petiole has 1.5-6 cm long. Leaves are oblong to ovate 5-19 cm long and 2.5-9 cm wide with slightly serrate margin and an acuminate tip. Both surfaces are scabrous, dark green above and lighter green beneath. Flowers are blue to violet and 6-8 cm in diameter trumpet-shaped as seen in figure 7.

In Thai traditional medicine, various part of *T. laurifolia* such as fresh and dried leaves, dried bark and root has been used for detoxification[12], anti-diabetic[36], anti-inflammatory[37], and antipyretic[38] properties. According to Thailand National List of Essential Medicines (NLEM), dried powder of *T. laurifolia* leaf has been used as single drug for antipyretic property and detoxification. Due to its detoxifying property, it has been excluded from combination drugs.

Figure 6 *Thunbergia laurifolia* Lindl. leaves

Figure 7 *Thunbergia laurifolia* Lindl. flowers

The quality control of *T. laurifolia* leaf has been evaluated in Thai Herbal Pharmacopoeia volume IV. The chemical constituents in the extract were evaluated by using repeatable high-performance liquid chromatography (HPLC) method. Oonsivilai et al[39] performed HPLC to evaluate chemical profile of various extracts including water, acetone, and ethanolic extracts from *T. laurifolia* leaf. The results indicated that fresh and dried leaf of various extracts contain phenolics, carotenoids and chlorophyll derivatives where chlorophyll derivatives found to be degraded through heating process. However, the HPLC solvent system developed in Oonsivilai et al research could not fractionate the water extract to elucidate the phenolics constituent in the extract.

Further phytochemical constituent analysis of *T. laurifolia* extract by HPLC method performed by Suwanchaikasem, Chaichantipyuth, and Sukrong found that rosmarinic acid (figure 8) is the major phenolic compound in the extract. They also evaluated an antioxidant activity of the extract with rosmarinic acid content by DPPH assay[14]. The antioxidant activity of the extract was correlated with the amount of rosmarinic acid content in the extract. Numerous studies[13, 15, 40, 41] have also indicated that rosmarinic acid is the major phenolic compound in *T. laurifolia* extract. Therefore, rosmarinic acid could be used as chemical marker for quantitative analysis of *T. laurifolia* extract. Interestingly, rosmarinic acid exhibited highest DPPH radical scavenging ability amongst ten different phenolic acids (figure 9) and positive controls like BHT and BHA at dose-dependent manner[42].

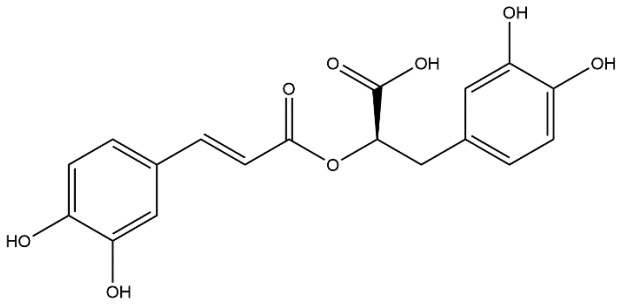

Figure 8 Chemical structure of rosmarinic acid

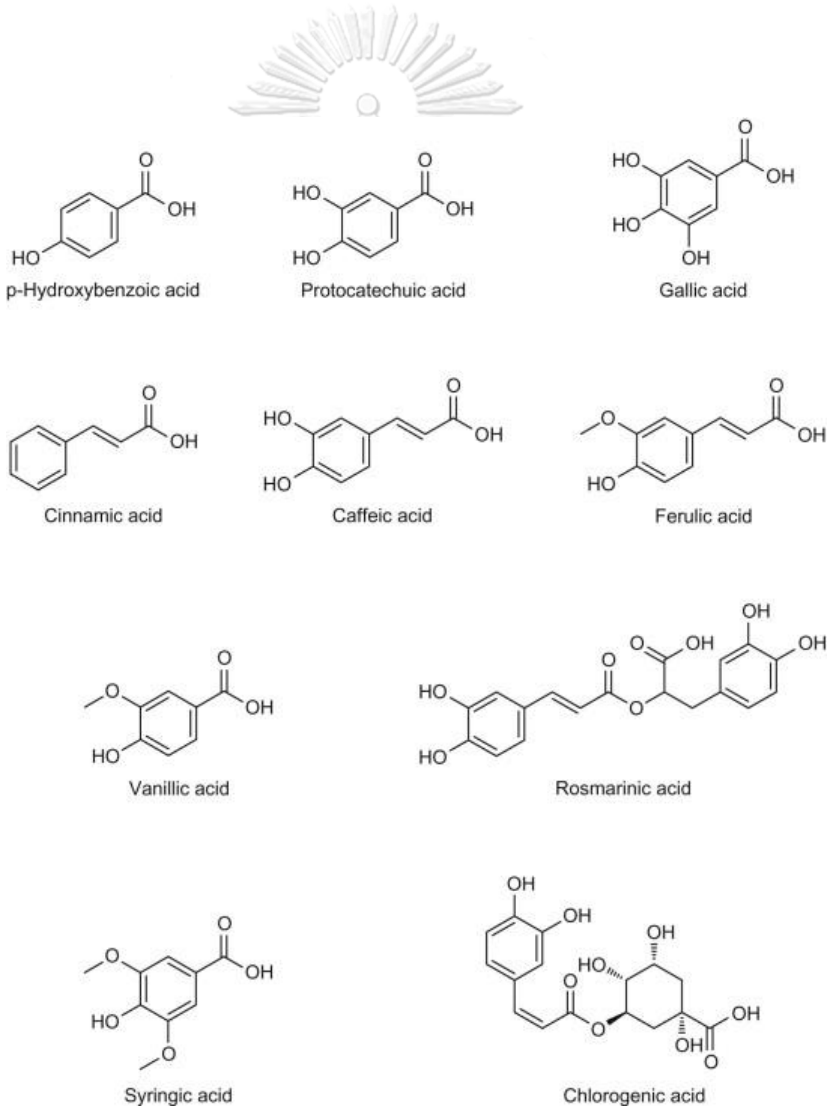

Figure 9 List of ten different phenolic compounds [42]

To conclude, the chemical profile of *T. laurifolia* water[13, 14, 39, 41, 43] and ethanolic[15, 16] extracts evaluated by various methods such as HPLC, liquid chromatography-mass spectrometry (LC-MS), and nuclear magnetic resonance spectroscopy (NMR) found phenolic compounds (rosmarinic acid and caffeic acid), flavonoid compounds (rutin, isoquercetin, quercetin, apigenin, and vitexin), polyphenol compound (catechin), organic compound (pyrogallol), and chlorophylls.

Recent HPLC-DAD method development by Woottisin et al[41] validated that the caffeic acid, rosmarinic acid, and vitexin chromatographic separation of *T. laurifolia* extract using developed mobile phase with constant flow rate at 1.0 mL/min, column controlled temperature at 25°C, and DAD detection wavelength at 330 nm was validated for its linearity, accuracy, precision, and limit of detection and quantitation. The developed and validated mobile phases consisted of 0.5% acetic acid in water (A) and methanol (B) with a gradient elution (A:B) as following steps: an initiation of solvent (A:B) 75:25 with a linear gradient to 35:65 in 15 min, followed by 100% solvent B for additional 20 min. The result concluded that rosmarinic acid is the major constituent following by caffeic acid, and the least amount of vitexin. Therefore, this study will perform HPLC analysis according to Woottisin et al[41] method for quantitative analysis of rosmarinic acid content in *T. laurifolia* ethanolic extract.

In addition, the stability of the three phenolic contents in the extract were also evaluated by five stress conditions including acid (37% w/w HCl at 60°C for 1 h)

and base (5 mol/L NaOH at 60°C for 1 h) hydrolytic, oxidative (30% w/w H_2O_2 at 60°C for 1 h), photolytic (light exposure at 4500 Lux for 72 h), and thermal (heat exposure at 80°C for 72 h) conditions in comparison to the control solvent (deionized water). Each forced stress sample was then analyzed % degradation of active compound by HPLC-DAD in the wavelength ranging from 200-400 nm. The results indicated that all three compounds were stable in oxidative condition and gradually degraded under accelerated condition at 40°C, 75% relative humidity. However, they were stable to store at room temperature up to 3 months. Moreover, the recent comparison of rosmarinic acid content in ethanolic extract and water extract of *T. laurifolia* shown that the ethanolic extract significantly contained higher rosmarinic acid the water extract, 5.26% ± 0.01% and 1.87% ± 0.02%, respectively[15].

The ethanolic extract of *T. laurifolia* leaf riches in rosmarinic acid has potent antioxidant activity. The extract exhibited scavenging effect against DPPH• radical and inhibitory effect against lipid peroxidation[15]. The extract could inhibit nitric oxide and inducible nitric oxide synthase (iNOS) production in LPS and IFN-γ-stimulated RAW264.7 mouse macrophage cells[16]. The extract could also inhibit ROS production and MMP-1 induced by H_2O_2 and UVA, respectively, in normal human dermal fibroblast cells[16].

CHAPTER III

METHODOLOGY

3.1 Materials and Samples preparation

3.1.1 Chemicals, reagents, and antibodies

Rosmarinic acid (96%), Dimethyl sulfoxide (DMSO), 2',7'-Dichlorodihydrofluorescein diacetate (H_2DCFDA) (≥ 97%), 3-(4,5-Dimethylthiazol-2-yl)-2,5-Diphenyltetrazolium Bromide (MTT), Hoechst 33342, Triton X-100, and paraformaldehyde were purchased from Sigma-Aldrich (St. Louis, MO, USA). Ethanol and glacial acetic acid were purchased from Merck KGaA (Darmstadt, Germany). Methanol (>99.9% HPLC grade) was purchased from Honeywell Burdick & Jackson (Muskegon, MI, USA). Dulbecco's modified eagle medium (DMEM) high glucose powder, fetal bovine serum (FBS), phosphate-buffered saline (PBS), trypsin-EDTA 0.25%, and Penicillin-Streptomycin were purchase from Gibco (Grand Island, NY, USA). RIPA lysis buffer, primary and secondary antibodies including CAT (#12980), GAPDH (#5174), Keap1 (#8047), SOD1 (#2770), SQSTM1/p62 (#5114), and anti-rabbit IgG (#7074) were obtained from Cell Signaling Technology (Danvers, MA, USA). Primary Nrf2 antibody (ab137550) was acquired from Abcam (Cambridge, UK). The secondary anti-rabbit antibodies for immunofluorescence including Alexa Fluor 488

(A-11034) and Alexa Fluor 594 (A-11037) were purchased from Invitrogen, Thermo Fisher (Eugene, OR, USA). The bovine serum albumin (BSA) and skim milk powder were purchased from Merck Millipore (HES, Germany). Sterile Polytetrafluoroethylene (PTFE) membrane syringe filters 0.22 μm and 0.45 μm were purchased from Chemplus (Jiangsu, China). Raw dried leaf of *T. laurifolia* lindl. was purchased from Ayurved Siriraj Manufacturing unit of Herbal Medicine and Products, Thailand.

3.1.2 $PM_{2.5}$ sampling and preparation

Urban $PM_{2.5}$ samples were collected 2.5 m away from Phaya Thai road located in Pathumwan district, Bangkok, Thailand (13°44'34.43"N 100°31'49.47"E). A set of Tisch Environmental TE-Wilbur Low Volume Air Particulate Sampler (Cleves, OH, USA) and OMNI FT Ambient Air Sampler (Lakewood, CO, USA) were used to collect $PM_{2.5}$ during May and June, 2021 with PTFE membrane filters with 46.2 mm in diameter and 2 μm pore size (figure 10). The collected sampling (figure 11) was then immersed in deionized water and sonicated using sonicator bath for 10 min prior to vortexed for another 10 min to extract $PM_{2.5}$ from PTFE filters. After that $PM_{2.5}$ suspensions were then lyophilized and weighed. The stock solution of $PM_{2.5}$ was prepared by resuspended lyophilized $PM_{2.5}$ in DMSO and kept at -20°C in the dark. The stock solution was then diluted with cell culture media to desired concentrations. The final non-toxic concentration of DMSO is less than 0.5% (v/v).

Figure 10 $PM_{2.5}$ collecting site

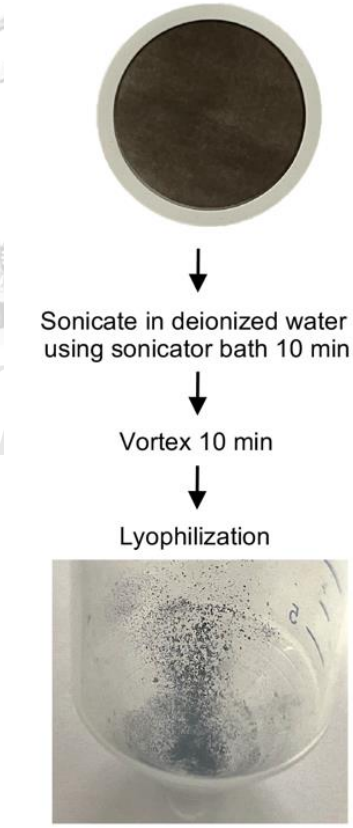

Figure 11 The flow chart of $PM_{2.5}$ preparation

3.2 Methods

3.2.1 Preparation of the *T. laurifolia* extract

Ground dried leaf (88 g) of *T. laurifolia* was macerated in 80% (v/v) ethanol at room temperature for 24 h. The extract was filtered, evaporated *in vacuo*, and lyophilized to obtain 9.22 g of crude ethanolic extract. The crude ethanolic extract were kept at -20°C in the dark. The stock solution of *T. laurifolia* extract (TLE) for biological assays was prepared by weighed, resuspended in DMSO, and filtered through sterile 0.45 µm and 0.22 µm PTFE syringe filters, respectively. The stock solution was then diluted with cell culture medium to desired concentrations with final concentration of DMSO less than 0.5% (v/v).

3.2.2 High-Performance Liquid Chromatography with Diode Array Detection (HPLC-DAD)

Rosmarinic acid content in *T. laurifolia* ethanolic extract was determined using HPLC-DAD. HPLC was performed using Agilent 1260 Infinity II LC system equipped with 1260 Quaternary pump, 1260 Multisampler, 1260 Multicolumn Thermostat, and 1260 DAD HS. Chromatography was achieved using Purospher® RP-18 endcapped HPLC column (250 cm x 4.6 mm, 5 µm) from Merck KGaA (Darmstadt, Germany) as a stationary phase. The mobile phases consisted of 0.5 % acetic acid in deionized water and methanol with a gradient elution according to Woottisin et al[41] method. A constant flow rate of 1.0 mL/min was conducted throughout the analysis

with temperature control at 25°C. The DAD detection wavelength was set at 330 nm. Reference standard rosmarinic acid and *T. laurifolia* extract were weighed at concentration of 1 mg/mL and 2 mg/mL, respectively. The samples were then dissolved in 50% methanol, and filtered through 0.22 µm PTFE syringe filter. Working solutions of standard rosmarinic acid were obtained by diluting the stock solution to desired concentrations of 31.25, 62.5, 125, 250, and 500 µg/mL. The injection volume was 10 µL. Each concentration was analyzed from triplicate injections. Calibration curve of reference standard rosmarinic acid was constructed by plotting various concentrations versus area under the curve. For method validation, linearity was determined by the correlation coefficient (R^2) of the calibration curve.

3.2.3 Cell culture

Human epidermal keratinocytes were obtained from CLS Cell Lines Services DmbH (#300493; Eppelheim, Germany). Keratinocytes were cultured in DMEM with high glucose (4.5 g/L) and 2 mM L-glutamine additives supplemented with 10% (v/v) FBS and 100 U/mL Penicillin-Streptomycin in a 37°C with 5% CO_2 humidified incubator.

3.2.4 Cell viability assay

Keratinocytes were seeded in 96-well plates at density of 1.3×10^4 cells/well and incubated at 37°C with 5% CO_2 overnight. After treatments, 0.5 mg/mL MTT solution was added and incubated at 37°C with 5% CO_2 for 4 h. Then formazan

crystals were solubilized with DMSO. The absorbance of formazan was measured at 570 nm using microplate reader (Anthros, Durham, NC, USA). The percentages of cell viability were calculated as the absorbance of treated cells relative to non-treated cells.

3.2.5 Intracellular ROS detection

Intracellular ROS production was detected using cell-permeable H_2DCFDA probe which diffused into cells and eventually enzymatically hydrolyzed by intracellular esterases to 2',7'-dichlorodihydrofluorescein (H_2DCF). In the presence of ROS, H_2DCF rapidly oxidized to 2',7'-dichlorofluorescein (DCF) which is highly fluorescent. Keratinocytes were seeded in 96-well plate at cell density of 1.8×10^4 cells/well and incubated at 37°C with 5% CO_2 overnight. Cells were washed with PBS prior to 10 μM H_2DCFDA probed for 30 min incubated at 37°C with 5% CO_2 in the dark. Excess H_2DCFDA were washed with PBS. The fluorescent intensity was measured using microplate reader CALIOstar from MBG Labtech GmbH (Ostenberg, Germany) with excitation and emission wavelength at 485 nm and 530 nm, respectively. The percentages of DCF fluorescent intensity were calculated as the fluorescent intensity of treated cells relative to non-treated cells.

3.2.6 Western Blot Analysis

Keratinocytes were seeded in 6-well plate at density of 4×10^5 cells/well and incubated at 37°C with 5% CO_2 overnight. After treatment, cells were collected and

lysed with RIPA lysis buffer for 30 min. Equivalent protein contents of each sample were separated by sodium dodecyl sulfate polyacrylamide gel electrophoresis (SDS-PAGE) followed by protein transferred to 0.2 μm polyvinylidene difluoride (PVDF) membranes from Bio-Rad (Hercules, CA, USA). After that, non-specific proteins on membranes were blocked with 5% skim milk in TBST for 1.5 h. Membranes were incubated with primary antibody specific to Nrf2, Keap1, p62, SOD, CAT, and GAPDH overnight at 4°C. Then, membranes were incubated with secondary anti-rabbit IgG antibody for 2 h at room temperature. The interested protein bands were detected using chemiluminescent substrate and exposed by Chemiluminescent ImageQuant LAS4000. Protein bands were then analyzed using ImageJ software version 1.53 by National Institutes of Health (Bethesda, MD, USA).

3.2.7 Immunofluorescence

Keratinocytes were seeded in 96-well plates at density of 1.2×10^4 cell/well and incubated at 37°C with 5% CO_2 overnight. After treatment, cells were fixed using 4% paraformaldehyde for 15 min, permeabilized using 0.5% Triton X for 5 min, and blocked with 10% FBS in 0.1% Triton X for an hour at room temperature. Cells were washed and incubated with specific antibodies for Nrf2 and p62 overnight at 4°C. Hoechst 33342 was added. Cells were visualized under fluorescent microscope (Olympus IX 51 with DP70) from Olympus America Inc. (Centervalley, PA, USA). The

quantitative analysis of fluorescent intensity was evaluated using ImageJ software version 1.53 by National Institutes of Health (Bethesda, MD, USA).

3.2.8 Statistical Analysis

All data were obtained from triplicate independent experiments. Values will be presented as mean ± standard error of the mean (SEM). The quantitative analysis of HPLC results were performed using Microsoft Excel software version 16.62. Statistical significances were analyzed using one-way analysis of variance (ANOVA) followed by Tukey's post hoc test. The p-value less than 0.05 was considered significant difference. SPSS software program version 28 (SPSS Inc., Chicago, IL, USA) was used. GraphPad Prism 9 by GraphPad Software (San Diego, CA, USA) was used to create graphs.

CHAPTER IV

RESULTS

4.1 Quantitative analysis of rosmarinic acid in *T. laurifolia* extract

HPLC-DAD analysis of ethanolic extract from *T. laurifolia* leaf was performed for quantitative analysis of major constituent, rosmarinic acid. The present HPLC-DAD method was validated as good precision as relative standard deviation (RSD) of every concentration injection < 2.0%. The representative HPLC chromatograms of standard rosmarinic acid and the extract were shown in figure 12-13, respectively. According to HPLC chromatogram of the extract, rosmarinic acid was detected at retention time approximately 15 min as seen in the reference standard chromatogram. The calibration curve of reference standard rosmarinic acid was reliable as the correlation coefficient (R^2) value 0.9999 (figure 14). The amount of rosmarinic acid content in the extract was calculated from reference standard calibration curve and triplicated injection of the extract. The quantity of rosmarinic acid in 1 mg of *T. laurifolia* extract (TLE) was calculated to be 62.59 ± 2.84 µg. The non-toxic concentration of *T. laurifolia* extract at 25, 50, and 100 µg/mL contained 1.56, 3.13, and 6.26 ± 2.84 µg rosmarinic acid, respectively.

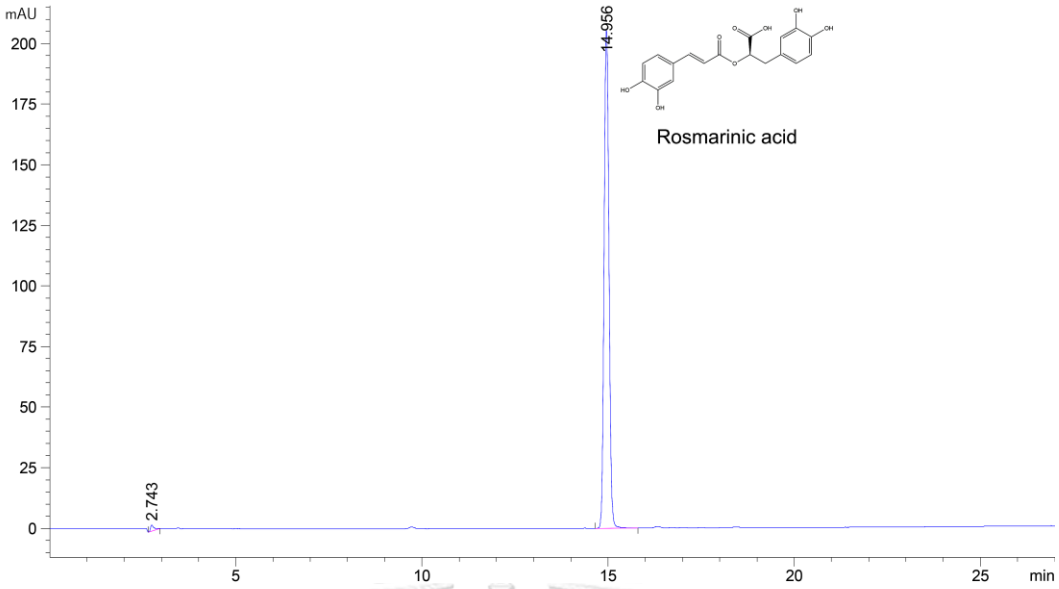

Figure 12 Representative chromatogram of rosmarinic acid

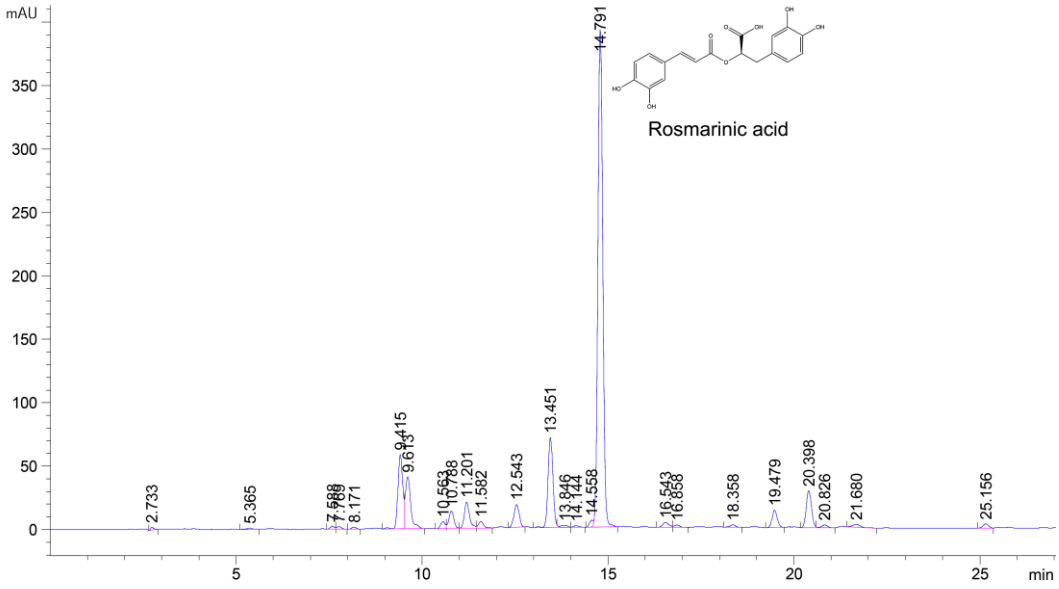

Figure 13 Representative chromatogram of *T. laurifolia* extract

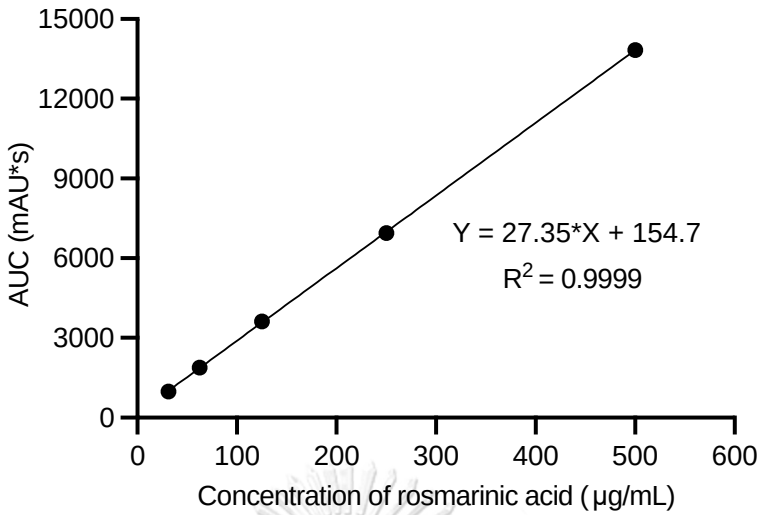

Figure 14 Calibration curve of reference standard rosmarinic acid

4.2 $PM_{2.5}$-induced oxidative stress in keratinocytes

Keratinocytes were treated with various concentrations (0-32 µg/mL) of $PM_{2.5}$ for 24 h. Figure 15 revealed that various concentrations of $PM_{2.5}$ had no significant toxic effect on cell viability. Consequently, various non-cytotoxic concentrations of $PM_{2.5}$ were monitored for ROS induction activity in keratinocytes using H_2DCFDA (figure 16). As a result, $PM_{2.5}$ at 16 µg/mL slightly increased ROS production while $PM_{2.5}$ at 32 µg/mL significantly induced ROS production 1.5-time of the non-treated control cells.

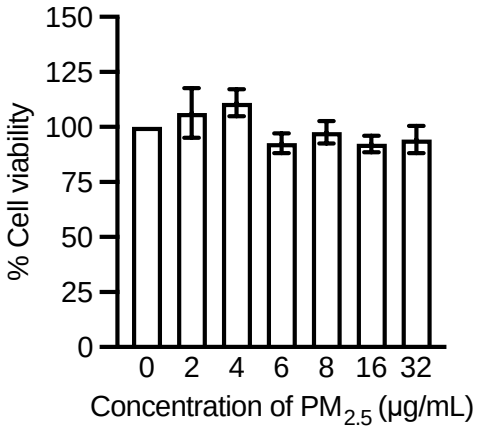

Figure 15 Effect of $PM_{2.5}$ on cell viability

To observe $PM_{2.5}$ effect on cell viability using MTT assay, keratinocytes were treated with various concentrations of TLE (0-400 µg/mL) for 24 h.

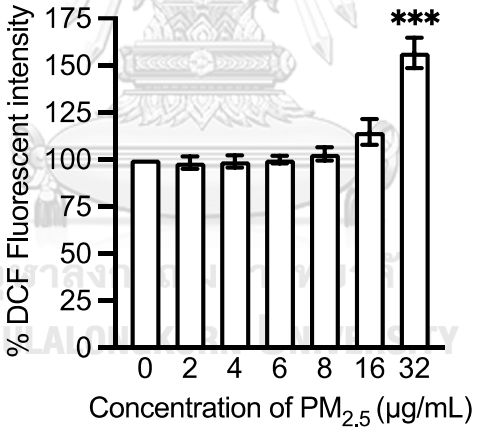

Figure 16 Intracellular ROS detection after $PM_{2.5}$ exposure for 6 h

After 6 h exposure to $PM_{2.5}$, keratinocytes were monitored ROS production by H_2DCFDA probe. Percentages of DCF fluorescent intensity were measured using microplate reader. All data were demonstrated as mean ± SEM (n=3). Asterisks denotes statistical differences between non-treatment and treatment. *** $p < 0.001$.

4.3 *T. laurifolia* extract inhibits $PM_{2.5}$-induced oxidative stress in keratinocytes

To elucidate maximum non-toxic concentration of TLE in keratinocytes, MTT assay was performed after 24 h treatment of various TLE concentrations (0-400 µg/mL). The result indicated that maximum non-cytotoxic concentration of TLE in keratinocytes was 150 µg/mL. However, the cell viability of treated cells at 150 µg/mL were notably decreased even not significance in comparison to the non-treatment control (figure 17). Further experiments using non-cytotoxic concentrations of TLE at 25, 50, and 100 µg/mL were proceeded.

To explore an antioxidant activity of TLE against $PM_{2.5}$-mediated oxidative stress induction, keratinocytes were co-treated with TLE (25, 50, and 100 µg/mL) and $PM_{2.5}$ (32 µg/mL) for 6 h in comparison to non-treated control and $PM_{2.5}$-treated cells. Intracellular ROS level was determined using H_2DCFDA (figure 18). The result depicted that TLE at 25, 50, and 100 µg/mL could significantly suppress ROS production in keratinocyte cells exposed to $PM_{2.5}$ from 130% to 89%, 89.7%, and 88.3%, respectively.

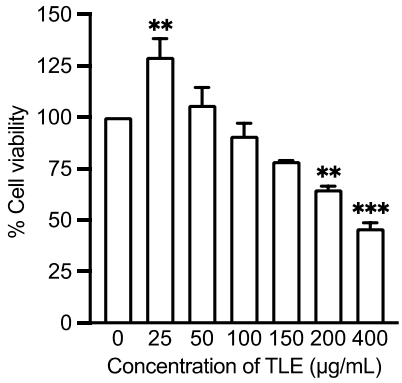

Figure 17 Effect of TLE on cell viability

To observe TLE effect on cell viability using MTT assay, keratinocytes were treated with various concentrations of TLE (0-400 µg/mL) for 24 h. Asterisks denotes statistical differences between groups (** $0.001 \leq p < 0.01$ and *** $p < 0.001$).

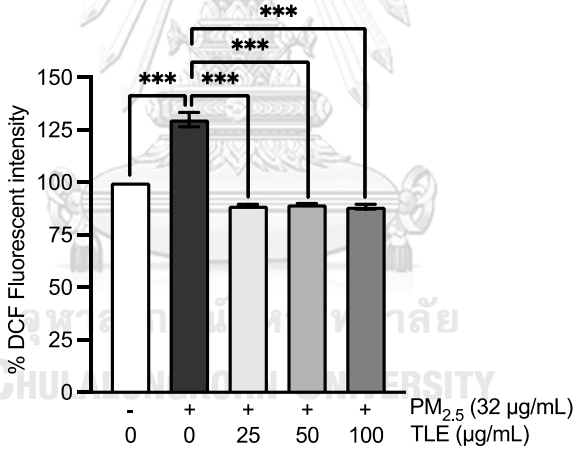

Figure 18 Intracellular ROS detection after 6 h of co-treatment

Keratinocytes were co-treated with TLE (0-100 µg/mL) and $PM_{2.5}$ (32 µg/mL) for 6 h in comparison to non-treatment and $PM_{2.5}$ treatment. Intracellular ROS production were detected using H_2DCFDA probe. Percentages of DCF fluorescent intensity were measured using microplate reader. Asterisks denotes statistical differences between groups (*** $p < 0.001$).

4.4 *T. laurifolia* extract induces the increase of cellular Nrf2 level

In order to evaluate the underlying mechanism, the Nrf2 protein was examined by western blot analysis (figure 19). Nrf2 of co-treated cells with various TLE concentrations (25, 50, and 100 µg/mL) were significantly increased at least two-fold in comparison to $PM_{2.5}$ treatment. Implying that TLE could suppress ROS in the cells via increasing the Nrf2 level.

Further, we elucidate whether TLE could enhance Nrf2 nuclear translocation and nuclear p62 expression. Keratinocytes were co-treated with TLE (25 and 100 µg/mL) and $PM_{2.5}$ (32 µg/mL) for 6 h in comparison to non-treatment and $PM_{2.5}$ treatment. According to figure 20, the co-treatment cells exhibited significantly upregulated nuclear Nrf2 expression in comparison to $PM_{2.5}$-treated cells. Interestingly, figure 21 depicted p62 up-regulation in the TLE-treated cells. As p62 is a protein regulating the Keap1, it may involve in the TLE-mediated Nrf2 increase.

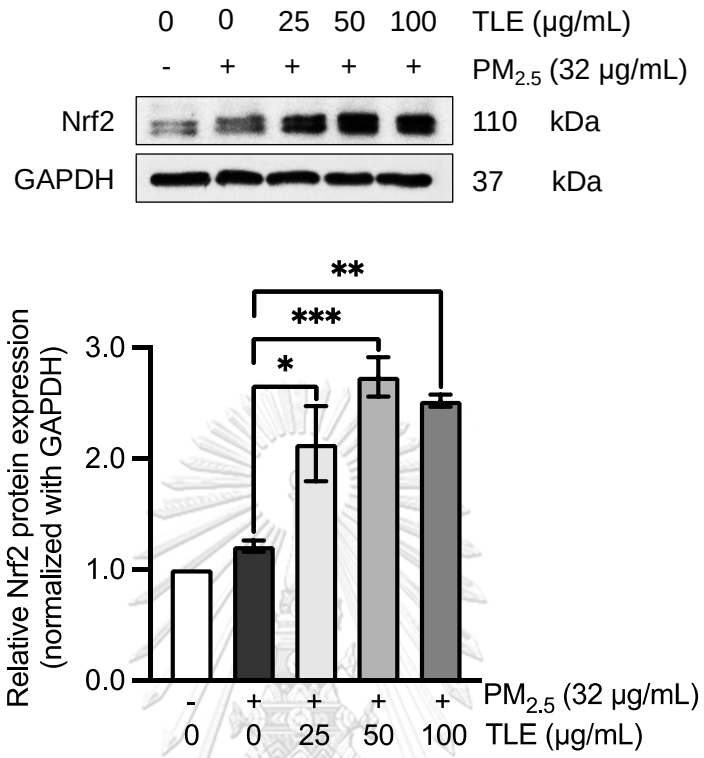

Figure 19 Western blot analysis of Nrf2 after 6 h of co-treatment

Effects of $PM_{2.5}$ and TLE co-treatment on Nrf2 activity in keratinocytes were evaluated by western blot analysis after 6 h treatment in comparison to non-treatment and $PM_{2.5}$ treatment. Densitometry of each protein levels were calculated, normalized with GAPDH, and represented in relative protein levels. Asterisks denotes statistical differences between groups (* $0.01 \leq p < 0.05$, ** $0.001 \leq p < 0.01$ and *** $p < 0.001$).

A

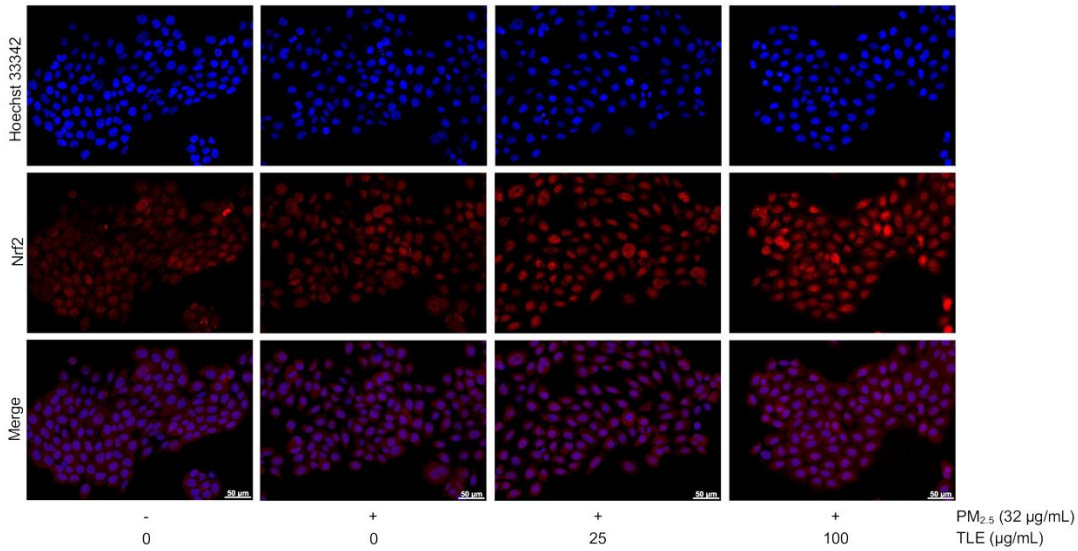

B

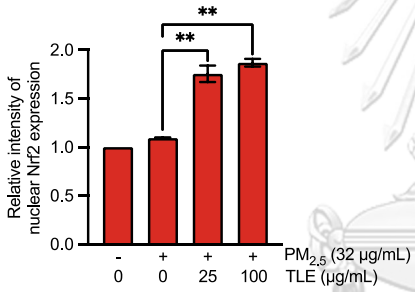

Figure 20 Immunofluorescence of Nrf2

Keratinocytes were co-treated with TLE (25 and 100 µg/mL) and $PM_{2.5}$ (32 µg/mL) for 6 h in comparison to non-treatment and $PM_{2.5}$ treatment.

(A) Immunofluorescence of Nrf2 was visualized under fluorescent microscope.

(B) The relative mean fluorescent intensity per cell was calculated.

All data were demonstrated as mean ± SEM (n=3). Asterisks denotes statistical differences between groups (** $0.001 \leq p < 0.01$).

A

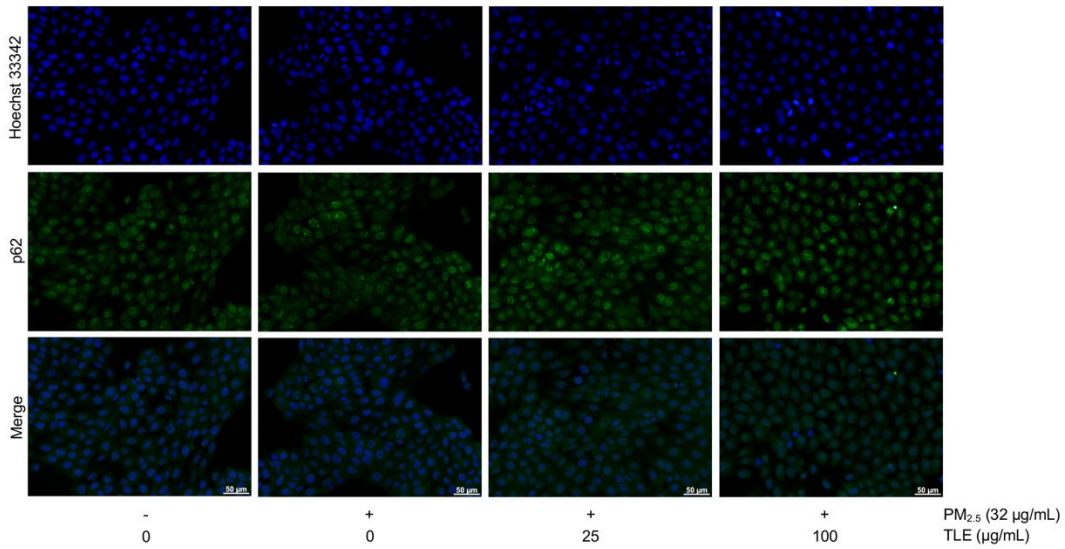

B

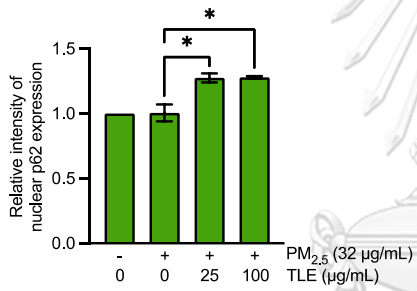

Figure 21 Immunofluorescence of p62

Keratinocytes were co-treated with TLE (25 and 100 µg/mL) and $PM_{2.5}$ (32 µg/mL) for 6 h in comparison to non-treatment and $PM_{2.5}$ treatment.

(A) Immunofluorescence of p62 was visualized under fluorescent microscope.

(B) The relative mean fluorescent intensity per cell was calculated.

All data were demonstrated as mean ± SEM (n=3). Asterisks denotes statistical differences between groups (* $0.01 \leq p < 0.05$).

4.5 Effect of *T. laurifolia* extract on cellular antioxidant defense system in keratinocytes

To confirm the mechanism of TLE on cellular antioxidant defense mechanism, cells were treated with TLE at 25, 50, and 100 µg/mL for 24 h and analyzed for the related proteins by western blot analysis. Protein expressions of interest including Nrf2, Keap1, p62, SOD and CAT were determined, and the protein levels were normalized with GAPDH level. According to figure 22, all TLE treatment could significantly upregulate Nrf2 and p62 expressions while decrease Keap1 level in dose-dependent manner. In addition, antioxidant SOD1 expression was also increased in TLE-treated cells in a dose-dependent manner. However, antioxidant CAT expression was unaltered. As p62 was shown to induced Keap1 degradation after it sequesters Keap1 from Nrf2-Keap1 dimer, these results suggested that TLE might, at least in part, activate Nrf2 through p62-dependent mechanism.

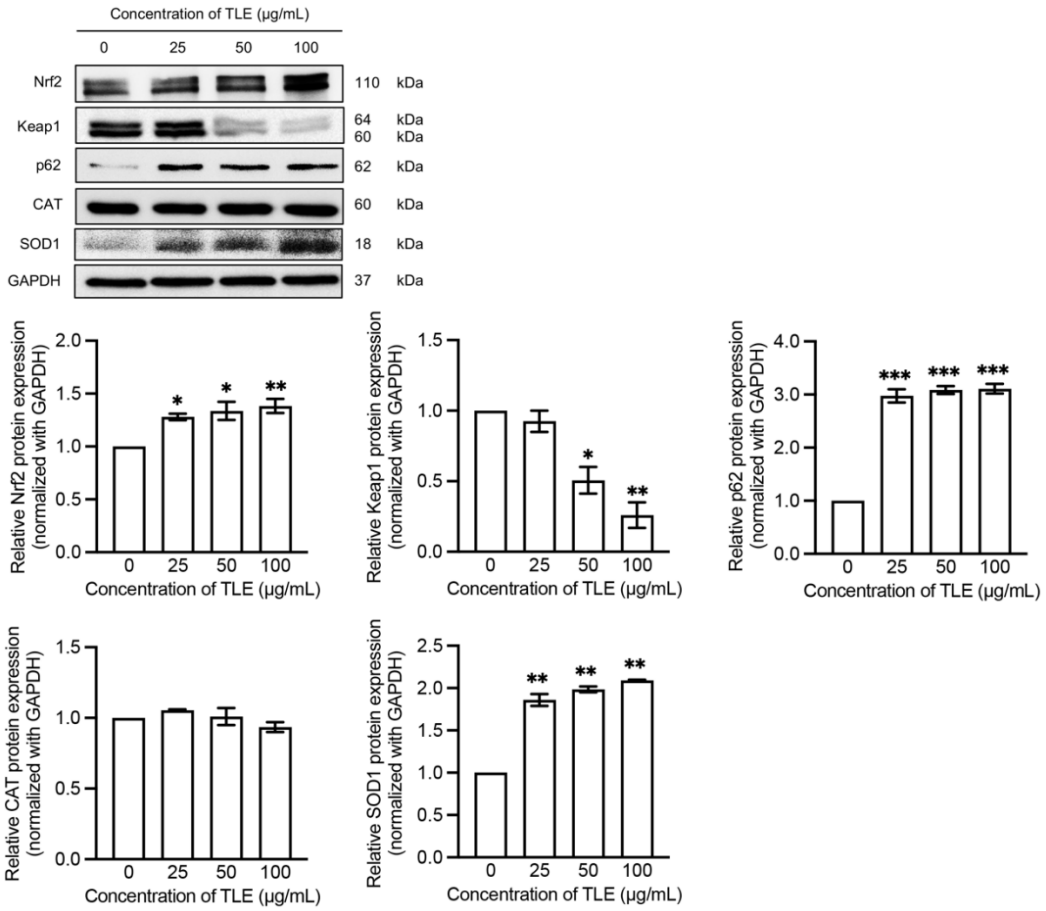

Figure 22 TLE regulates p62-Keap1-Nrf2 signaling pathway in keratinocytes

Keratinocytes were treated with various concentrations of TLE (0-100 μg/mL) for 24 h. Protein expressions related to p62-Keap1-Nrf2 signaling pathway were evaluated using western blot analysis. Densitometry of each protein levels were calculated, normalized with GAPDH, and represented in relative protein levels. Asterisks denotes statistical differences between non-treatment and treatment (* $0.01 \leq p < 0.05$, ** $0.001 \leq p < 0.01$ and *** $p < 0.001$).

CHAPTER V

DISCUSSION

The organic and inorganic compounds (mainly PAHs and metals, respectively) in $PM_{2.5}$ can damage cellular mitochondria resulting in excess ROS generation[44]. As keratinocytes constantly expose to $PM_{2.5}$, excess ROS generation could lead to oxidative stress and apoptosis[35]. In this study, the exposure of $PM_{2.5}$ could significantly induce intracellular ROS production in keratinocytes in such a short period of time (figure 16). Although chosen concentration of $PM_{2.5}$ (32 µg/mL) had no significant effect on cell viability (figure 15), the remarkably increase in intracellular ROS production validated its potential damage to keratinocytes. Although $PM_{2.5}$ solution was heterogenous, the cell-permeable components of $PM_{2.5}$ enabling cell penetration during exposure in keratinocytes.

Potent antioxidants could inhibit oxidative stress[9]. The ethanolic extract of *T. laurifolia* leaf riches in rosmarinic acid has potent antioxidant activity. The extract has scavenging effect against $DPPH^{\bullet}$ radical and inhibitory effect against lipid peroxidation[15]. It can inhibit nitric oxide and inducible nitric oxide synthase (iNOS) production in LPS and IFN-**γ**-stimulated RAW264.7 mouse macrophage cells[16]. The extract could also inhibit ROS production and MMP-1 induced by H_2O_2 and UVA, respectively, in normal human dermal fibroblast cells[16]. Furthermore, the extract

has potent anti-aging activity as it also inhibits MMP-2, and MMP-9 in albino swiss mouse embryo fibroblasts 3T3 cells[15]. Interestingly, the extract could inhibit glutamate-induced neurotoxicity and cell death through autophagy and mitophagy mechanisms in mouse hippocampal neuronal HT-22 cells[45]. The results in this study demonstrated that TLE is a potent natural antioxidant. In co-treatment condition, TLE effectively maintained cellular redox homeostasis comparing to the non-treatment during 6 h of $PM_{2.5}$ exposure (figure 18). In the presence of TLE, excess ROS generation was dramatically suppressed in comparison to $PM_{2.5}$ treatment. The ROS scavenging effect of TLE at 25-100 µg/mL were more than enough to counteract the $PM_{2.5}$-induced oxidative stress. During this 6 h of co-treatment, TLE did not transactivate antioxidant and detoxifying enzymes yet. Nrf2 and p62 were notably activated by TLE according to western blot and immunofluorescent results as seen in figures 19-21.

Autophagy is a crucial detoxifying mechanism mediating nrf2 activity through p62-Keap1-Nrf2 signaling pathway[11]. An autophagic process of p62-Keap1 complex enable nrf2 to activate[10]. According to the 24 h TLE treatment (figure 22), the decrease in Keap1 expression might result from autophagic degradation which contradict to upregulated p62. Activated Nrf2 might transactivate p62 gene in positive feedback mechanism of p62-Keap1-Nrf2 signaling pathway[46]. On the other hand, the immunofluorescence of p62 (figure 21) depicted p62 accumulation in the nucleus. The nuclear p62 accumulation might result from nuclear proteasomal degradation.

The proteasomal degradation of protein complex by ubiquitin-proteasome system (UPS) required many components recruitment such as ubiquitin, ubiquitin ligases (E1-E3), ubiquitin moiety, and proteasome[47]. Recent study found that nuclear accumulation complex containing p62 as an essential component which accelerate the recruitment of UPS and protein substrates facilitating the degradation in both normal and stimulated states[48].

Moreover, an underlying cellular defense system of TLE in keratinocytes was validated. According to western blot analysis after 24 h treatment (figure 22), TLE non-canonical activated Nrf2 with p62 mediation. The upregulated p62 might sequester Keap1 from Nrf2-Keap1 dimer and undergoes autophagic degradation[10]. The upregulation of Nrf2, p62, and SOD1 expressions might result from antioxidant and detoxifying genes transactivation by Nrf2 in the nucleus[11]. In summary, TLE regulating p62-Keap1-Nrf2 signaling pathway in order to maintain cellular redox against $PM_{2.5}$-induced oxidative stress in keratinocytes (figure 23).

To conclude, TLE possesses antioxidant activity against $PM_{2.5}$-induced oxidative stress in keratinocytes. The findings in this study support the potential application of TLE as natural antioxidants in cosmetic and pharmaceutical industry.

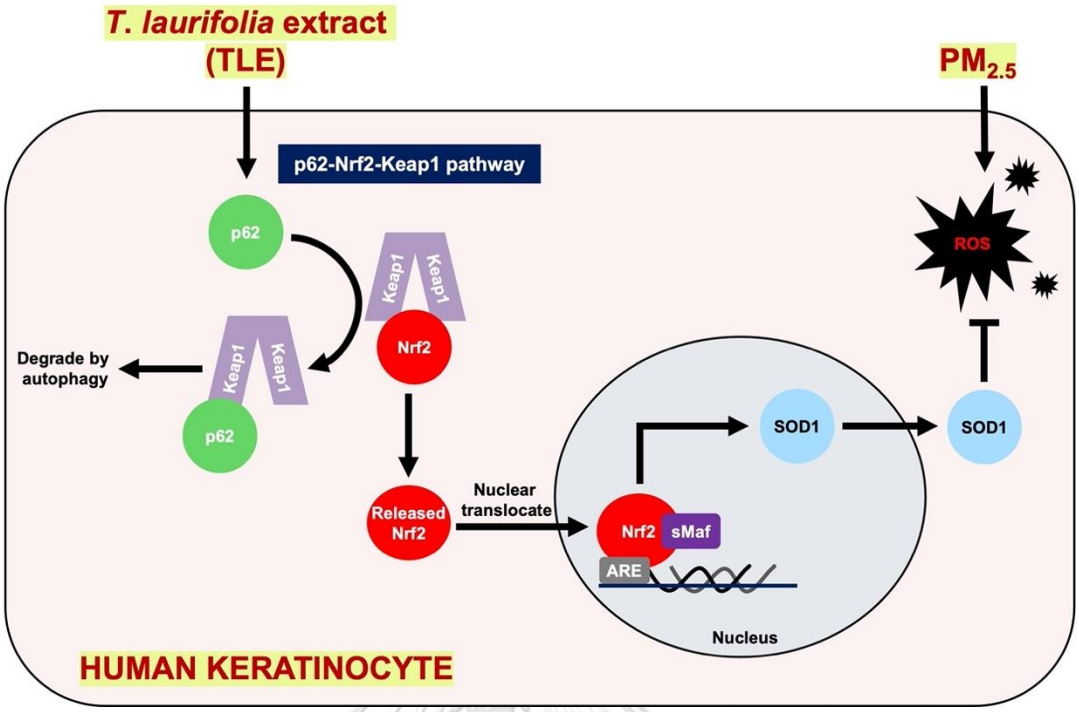

Figure 23 TLE inhibits $PM_{2.5}$-induced oxidative stress by regulating p62-Keap1-Nrf2 signaling pathway in human keratinocyte

The upregulated p62 sequestered Keap1 from Nrf2-Keap1 dimer and degraded by autophagy. The released Nrf2 was then translocated into nucleus, formed heterodimer with small Maf proteins (sMaf), and bound with antioxidant responsive elements (ARE) to transactivate target genes including SOD1. The increased SOD1 counteracts excessive ROS production induced by $PM_{2.5}$ exposure.

REFERENCES

1. Honari G. Skin structure and function. Sensitive Skin Syndrome: CRC Press; 2017. p. 16-22.

2. Yousef H, Alhajj M, Sharma S. Anatomy, skin (integument), epidermis. 2017.

3. Raihana Nazirah Roslan T, Rukayyah Al-Munirah Ayob M, Yi Sean O, Zainuddin N. RISK OF AIR POLLUTION FROM INDUSTRIALIZATION TOWARDS HEALTH: A COMPARATIVE RISK ASSESSMENT. EDPACS. 2022;65(5):1-16.

4. Manisalidis I, Stavropoulou E, Stavropoulos A, Bezirtzoglou E. Environmental and Health Impacts of Air Pollution: A Review. Frontiers in Public Health. 2020;8(14).

5. Tian Y, Liu X, Huo R, Shi Z, Sun Y, Feng Y, et al. Organic compound source profiles of PM2. 5 from traffic emissions, coal combustion, industrial processes and dust. Chemosphere. 2021;278:130429.

6. Fitoussi R, Faure M-O, Beauchef G, Achard S. Human skin responses to environmental pollutants: A review of current scientific models. Environmental Pollution. 2022:119316.

7. Dijkhoff IM, Drasler B, Karakocak BB, Petri-Fink A, Valacchi G, Eeman M, et al. Impact of airborne particulate matter on skin: A systematic review from epidemiology to in vitro studies. Particle and fibre toxicology. 2020;17(1):1-28.

8. Gęgotek A, Skrzydlewska E. The role of transcription factor Nrf2 in skin cells metabolism. Archives of Dermatological Research. 2015;307(5):385-96.

9. Boo YC. Natural Nrf2 modulators for skin protection. Antioxidants. 2020;9(9):812.

10. Katsuragi Y, Ichimura Y, Komatsu M. Regulation of the Keap1–Nrf2 pathway by p62/SQSTM1. Current Opinion in Toxicology. 2016;1:54-61.

11. Jiang T, Harder B, De La Vega MR, Wong PK, Chapman E, Zhang DD. p62 links autophagy and Nrf2 signaling. Free Radical Biology and Medicine. 2015;88:199-204.

12. Chattaviriya P, Morkmek N, Lertprasertsuke N, Ruangyuttikarn W. Drinking Thunbergia laurifolia Lindl. leaf extract helps prevent renal toxicity induced by cadmium in rats. Thai Journal of Toxicology. 2010;25(2):124-.

13. Junsi M, Siripongvutikorn S. Thunbergia laurifolia, a traditional herbal tea of

Thailand: botanical, chemical composition, biological properties and processing influence. International Food Research Journal. 2016;23(3):923.

14. Suwanchaikasem P, Chaichantipyuth C, Sukrong S. Antioxidant-guided isolation of rosmarinic acid, a major constituent from Thunbergia laurifolia, and its use as a bioactive marker for standardization. Chiang Mai J Sci. 2014;41(1):117-27.

15. Chaiyana W, Chansakaow S, Intasai N, Kiattisin K, Lee K-H, Lin W-C, et al. Chemical Constituents, Antioxidant, Anti-MMPs, and Anti-Hyaluronidase Activities of Thunbergia laurifolia Lindl. Leaf Extracts for Skin Aging and Skin Damage Prevention. Molecules. 2020;25(8):1923.

16. Pattananandecha T, Apichai S, Julsrigival J, Ungsurungsie M, Samuhasaneetoo S, Chulasiri P, et al. Antioxidant Activity and Anti-Photoaging Effects on UVA-Irradiated Human Fibroblasts of Rosmarinic Acid Enriched Extract Prepared from Thunbergia laurifolia Leaves. Plants. 2021;10(8):1648.

17. Hoath SB, Leahy D. The organization of human epidermis: functional epidermal units and phi proportionality. Journal of Investigative Dermatology. 2003;121(6):1440-6.

18. Lee D, Ashcraft JN, Verploegen E, Pashkovski E, Weitz DA. Permeability of model stratum corneum lipid membrane measured using quartz crystal microbalance. Langmuir. 2009;25(10):5762-6.

19. Seneschal J, Clark RA, Gehad A, Baecher-Allan CM, Kupper TS. Human epidermal Langerhans cells maintain immune homeostasis in skin by activating skin resident regulatory T cells. Immunity. 2012;36(5):873-84.

20. Prost-Squarcioni C, Fraitag S, Heller M, Boehm N, editors. Functional histology of dermis. Annales de dermatologie et de venereologie; 2008.

21. Yang G, Seok JK, Kang HC, Cho Y-Y, Lee HS, Lee JY. Skin barrier abnormalities and immune dysfunction in atopic dermatitis. International journal of molecular sciences. 2020;21(8):2867.

22. Wlaschek M, Tantcheva-Poór I, Naderi L, Ma W, Schneider LA, Razi-Wolf Z, et al. Solar UV irradiation and dermal photoaging. Journal of Photochemistry and Photobiology B: Biology. 2001;63(1-3):41-51.

23. Itoh K, Chiba T, Takahashi S, Ishii T, Igarashi K, Katoh Y, et al. An Nrf2/small Maf heterodimer mediates the induction of phase II detoxifying enzyme genes through

antioxidant response elements. Biochemical and biophysical research communications. 1997;236(2):313-22.

24. Itoh K, Wakabayashi N, Katoh Y, Ishii T, O'Connor T, Yamamoto M. Keap1 regulates both cytoplasmic-nuclear shuttling and degradation of Nrf2 in response to electrophiles. Genes to cells. 2003;8(4):379-91.

25. Natsch A. The Nrf2-Keap1-ARE toxicity pathway as a cellular sensor for skin sensitizers—functional relevance and a hypothesis on innate reactions to skin sensitizers. Toxicological Sciences. 2010;113(2):284-92.

26. Keum Y-S. Regulation of Nrf2-mediated phase II detoxification and anti-oxidant genes. Biomolecules & Therapeutics. 2012;20(2):144.

27. Auf dem Keller U, Huber M, Beyer TA, Kumin A, Siemes C, Braun S, et al. Nrf transcription factors in keratinocytes are essential for skin tumor prevention but not for wound healing. Molecular and cellular biology. 2006;26(10):3773-84.

28. Mancebo S, Wang S. Recognizing the impact of ambient air pollution on skin health. Journal of the European Academy of Dermatology and Venereology. 2015;29(12):2326-32.

29. Fridovich I. Superoxide anion radical (O· 2), superoxide dismutases, and related matters. Journal of Biological Chemistry. 1997;272(30):18515-7.

30. Schieber M, Chandel NS. ROS function in redox signaling and oxidative stress. Current biology. 2014;24(10):R453-R62.

31. WHO. Ambient (outdoor) air pollution 2021 [22 September 2021:[Available from: https://www.who.int/news-room/fact-sheets/detail/ambient-(outdoor)-air-quality-and-health.

32. Adams K, Greenbaum DS, Shaikh R, van Erp AM, Russell AG. Particulate matter components, sources, and health: Systematic approaches to testing effects. Journal of the Air & Waste Management Association. 2015;65(5):544-58.

33. Magnani ND, Muresan XM, Belmonte G, Cervellati F, Sticozzi C, Pecorelli A, et al. Skin damage mechanisms related to airborne particulate matter exposure. Toxicological sciences. 2016;149(1):227-36.

34. Jin S-P, Li Z, Choi EK, Lee S, Kim YK, Seo EY, et al. Urban particulate matter in air

pollution penetrates into the barrier-disrupted skin and produces ROS-dependent cutaneous inflammatory response in vivo. Journal of dermatological science. 2018;91(2):175-83.

35. Pardo M, Qiu X, Zimmermann R, Rudich Y. Particulate matter toxicity is Nrf2 and mitochondria dependent: the roles of metals and polycyclic aromatic hydrocarbons. Chemical research in toxicology. 2020;33(5):1110-20.

36. Aritajat S, Wutteerapol S, Saenphet K. Anti-diabetic effect of Thunbergia laurifolia Linn. aqueous extract. Southeast Asian J Trop Med Public Health. 2004;35(Suppl 2):53-8.

37. Boonyarikpunchai W, Sukrong S, Towiwat P. Antinociceptive and anti-inflammatory effects of rosmarinic acid isolated from Thunbergia laurifolia Lindl. Pharmacology Biochemistry and Behavior. 2014;124:67-73.

38. Nanna U, Chiruntanat N, Jaijoy K, Rojsanga P, Sireeratawong S. Effect of Thunbergia laurifolia Lindl. Extract on Anti-Inflammatory, Analgesic and Antipyretic Activity. JOURNAL OF THE MEDICAL ASSOCIATION OF THAILAND. 2017;100(6):98.

39. Oonsivilai R, Cheng C, Bomser J, Ferruzzi MG, Ningsanond S. Phytochemical profiling and phase II enzyme-inducing properties of Thunbergia laurifolia Lindl.(RC) extracts. Journal of Ethnopharmacology. 2007;114(3):300-6.

40. Ruangpayungsak N, Sithisarn P, Rojsanga P. High performance liquid chromatography fingerprinting and chemometric analysis of antioxidant quality of Thunbergia laurifolia leaves. Journal of Liquid Chromatography & Related Technologies. 2018;41(11):713-21.

41. Woottisin N, Kongkiatpaiboon S, Sukprasert S, Sathirakul K. Development and Validation of Stability Indicating HPLC Method for Determination of Caffeic Acid, Vitexin and Rosmarinic Acid in Thunbergia laurifolia Leaf Extract. Pharmacognosy Journal. 2020;12(3).

42. Sevgi K, Tepe B, Sarikurkcu C. Antioxidant and DNA damage protection potentials of selected phenolic acids. Food and Chemical Toxicology. 2015;77:12-21.

43. Rojsanga P, Sithisarn P, Sanguansataya T. Simultaneous determination of caffeic acid and vitexin contents in Thunbergia laurifolia leaf extracts collected from different provinces in Thailand by HPLC. Pharm Sci Asia. 2018;45(4):205-12.

44. Shuster-Meiseles T, Shafer MM, Heo J, Pardo M, Antkiewicz DS, Schauer JJ, et al. ROS-generating/ARE-activating capacity of metals in roadway particulate matter deposited in urban environment. Environmental research. 2016;146:252-62.

45. Vongthip W, Sillapachaiyaporn C, Kim K-W, Sukprasansap M, Tencomnao T. Thunbergia laurifolia Leaf Extract Inhibits Glutamate-Induced Neurotoxicity and Cell Death through Mitophagy Signaling. Antioxidants. 2021;10(11):1678.

46. Sánchez‐Martín P, Saito T, Komatsu M. p62/SQSTM 1:'Jack of all trades' in health and cancer. The FEBS journal. 2019;286(1):8-23.

47. Liu WJ, Ye L, Huang WF, Guo LJ, Xu ZG, Wu HL, et al. p62 links the autophagy pathway and the ubiqutin–proteasome system upon ubiquitinated protein degradation. Cellular & molecular biology letters. 2016;21(1):1-14.

48. Fu A, Cohen-Kaplan V, Avni N, Livneh I, Ciechanover A. p62-containing, proteolytically active nuclear condensates, increase the efficiency of the ubiquitin–proteasome system. Proceedings of the National Academy of Sciences. 2021;118(33):e2107321118.

VITA

NAME	Buakotchaphan Jirabanjerdsiri
DATE OF BIRTH	13 Feb 1997
PLACE OF BIRTH	Bangkok, Thailand
INSTITUTIONS ATTENDED	Mahidol University
HOME ADDRESS	1298/1045 Rama 3 road Chongnonsi Yannawa Bangkok, Thailand 10120
PUBLICATION	-
AWARD RECEIVED	-